Electronic, magnetic and optical properties of two Fe-based superconductors and related parent compounds

2010 Supercond. Sci. Technol. 23 054005

(http://iopscience.iop.org/0953-2048/23/5/054005)

Supercond. Sci. Technol. **23** (2010) 054005 (6pp) doi:10.1088/0953-2048/23/5/054005

Electronic, magnetic and optical properties of two Fe-based superconductors and related parent compounds

R Jin[1], M H Pan[2], X B He[1], Guorong Li[1], De Li[3], Ru-wen Peng[3], J R Thompson[2,4], B C Sales[2], A S Sefat[2], M A McGuire[2], D Mandrus[2,5], J F Wendelken[2], V Keppens[5] and E W Plummer[1]

[1] Department of Physics and Astronomy, Louisiana State University, Baton Rouge, LA 70803, USA
[2] Oak Ridge National Laboratory, Oak Ridge, TN 37831, USA
[3] National Laboratory of Solid State Microstructures and Department of Physics, Nanjing University, 210093, People's Republic of China
[4] Department of Physics and Astronomy, The University of Tennessee, Knoxville, TN 37996, USA
[5] Department of Materials and Engineering, The University of Tennessee, Knoxville, TN 37996, USA

E-mail: rjin@lsu.edu

Received 15 December 2009, in final form 9 March 2010
Published 23 April 2010
Online at stacks.iop.org/SUST/23/054005

Abstract
We have investigated the electronic, magnetic, and optical properties of two Fe-based superconductors and related parent compounds via three powerful techniques: scanning tunneling microscopy/spectroscopy (STM/S), high-temperature vibrating sample magnetometry, and optical transmission spectroscopy (OTS). Below the superconducting transition temperature $T_c \sim 48$ K, the STM/S of polycrystalline $NdFeAsO_{0.86}F_{0.14}$ reveals a single-gap feature. The quantitative fitting of STS data results in Bardeen–Cooper–Schrieffer-like temperature dependence of the energy gap $\Delta(T)$, with $2\Delta(0)/k_BT_c \sim 4.3$. The tunneling spectra of $BaFe_2As_2$ single crystals show no evidence for the opening of a gap below the magnetic/structural transition temperature $T_{MS} \sim 140$ K. This transition also had little impact on the transmission spectra in the wavelength range between 400 and 2400 nm. But its effect on the magnetic properties is dramatic, as reflected in the unusual magnetic susceptibility over a wide temperature range.

(Some figures in this article are in colour only in the electronic version)

1. Introduction

The discovery of superconductivity in iron (Fe)-based compounds has generated enormous excitement because they are the first copper-free superconductors with T_c exceeding 55 K [1–6]. This new class of materials has stimulated broad speculation on the origin of electron pairing in the superconducting state. At first glance, they have been advertised as the 'cousins' of high-T_c cuprates, due to their layered structures with either FeAs or FeSe/Te as building blocks. The accumulation of two-years of experimental and theoretical investigations indicates that Fe-based superconductors are unique in their own right: (1) co-valent bonding within layers with Fe in a tetrahedral environment, (2) great chemical flexibility allowing the partial substitutions of Fe by other magnetic elements [7–10], (3) small anisotropy in physical properties in spite of the layered structure [11–14], (4) metallic ground states of their parent compounds [1–6], and (5) multi-band nature in their electronic structures [15–17]. These characteristics

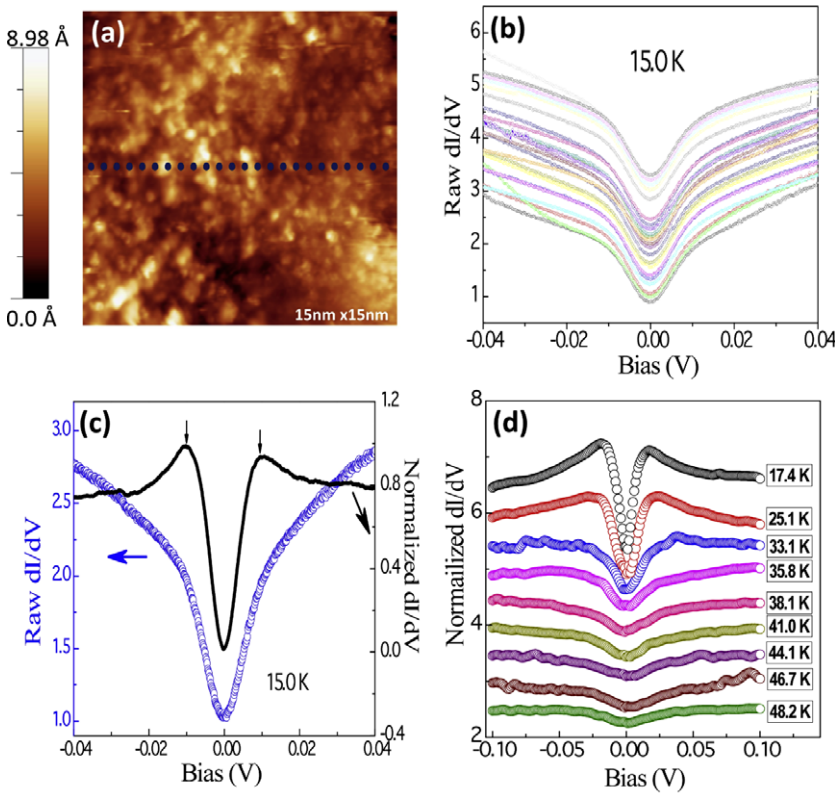

Figure 1. (a) Constant current STM image shows the surface corrugation of an $NdFeAsO_{0.86}F_{0.14}$ sample within a 15 × 15 nm^2 scanning range at 15 K. The bias is 100 mV, and the current is 100 pA; (b) tunneling spectra at 15 K taken at locations as indicated by black dots in (a); (c) comparison of the raw STS data (blue empty circles) with the normalized dI/dV (black curve); and (d) temperature dependence of normalized dI/dV spectra below T_c of $NdFeAsO_{0.86}F_{0.14}$.

likely reflect different underlying physics in Fe-based superconductors compared to CuO_2-based superconductors.

In this article, we report experimental results obtained from optimally doped superconducting $NdFeAsO_{0.86}F_{0.14}$ and $Ba(Fe_{0.9}Co_{0.1})_2As_2$, and related parent compounds $BaFe_2As_2$, $SrFe_2As_2$. For polycrystalline $NdFeAsO_{0.86}F_{0.14}$, our high-resolution scanning tunneling microscopy/spectroscopy (STM/S) was employed to study the temperature and location dependence of the electronic density of states (DOS). While spatial variations are observed, all STS curves reveal a single-gap feature below T_c. The quantitative fitting of STS data to the Dynes function results in BCS-like temperature dependence of the energy gap $\Delta(T)$, with $2\Delta(0)/k_BT_c \sim 4.3$. An attempt was also made to study the electronic structure of $BaFe_2As_2$, because the spin-density-wave (SDW) state is usually associated with the opening of the energy gap at the Fermi surface. Despite the clean surface with atomic resolution, the STS of $BaFe_2As_2$ provides a gapless character below the magnetic/structural transition T_{MS}. Similarly, the optical transmission spectroscopy (OTS) of $BaFe_2As_2$ remains more or less the same in the wavelength range between 400 and 2400 nm when crossing T_{MS}. A possible origin is discussed by comparing the OTS data with that for superconducting $Ba(Fe_{0.9}Co_{0.1})_2As_2$. Following earlier work that showed an unusual temperature dependence of the magnetic susceptibility (χ) in both parent compounds and superconductors [18], we now extend the measurements for $BaFe_2As_2$ and $SrFe_2As_2$ single crystals up to 700 K, using both superconducting quantum interference device (SQUID) and vibrating sample magnetometers by *Quantum Design*. Remarkably, the magnetic susceptibility, above T_{MS}, increases rather linearly with increasing T up to at least 700 K, without any sign of a turnaround. Such behavior is very similar to that seen in chromium (Cr) metal.

2. Experimental results and discussion

2.1. Scanning tunneling microscopy/spectroscopy of superconducting $NdFeAsO_{0.86}F_{0.14}$ and $BaFe_2As_2$

Polycrystalline $NdFeAsO_{0.86}F_{0.14}$ and single-crystalline $SrFe_2As_2$, $BaFe_2As_2$ and $Ba(Fe_{0.9}Co_{0.1})_2As_2$ were prepared via solid-state reaction and flux methods with the details described elsewhere [7, 18, 19]. Both electrical resistivity and magnetic susceptibility measurements indicate that $NdFeAsO_{0.86}F_{0.14}$ undergoes superconducting transition at $T_c = 48$ K (90% drop in electrical resistivity). The structural/magnetic transition occurs in $BaFe_2As_2$ at $T_{MS} \sim 140$ K [7]. For STM/S measurements, samples were placed in ultrahigh vacuum (base pressure $< 3 \times 10^{-11}$ Torr), and either scraped ($NdFeAsO_{0.86}F_{0.14}$) or cleaved ($BaFe_2As_2$) at liquid nitrogen temperature to obtain a clean and fresh surface.

Figure 1(a) shows a typical STM image of the scraped $NdFeAsO_{0.86}F_{0.14}$ surface taken at the tunneling current of 100 pA. Note that the surface is reasonably flat with corrugation less than 1 nm in the area of 15 nm × 15 nm. As might be expected, this scraped surface does not display an

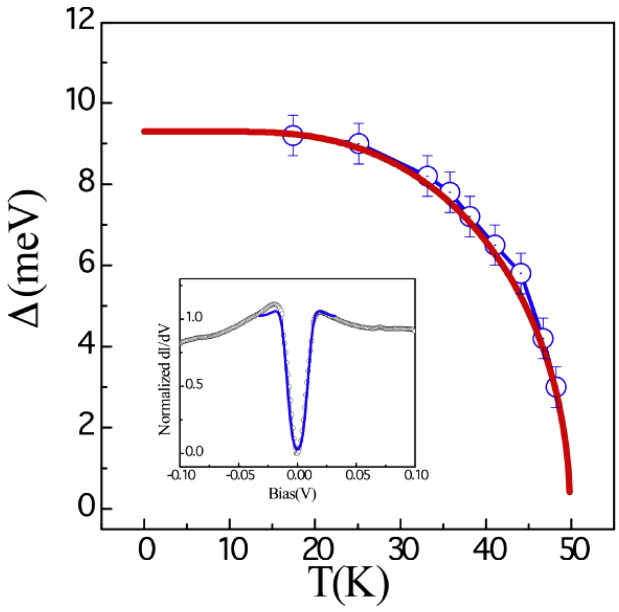

Figure 2. Temperature dependence of the superconducting gap value (open circles) obtained from the fit of our STS data to the Dynes function. The error bar is due to the fitting. The red curve represents BCS-like temperature dependence of Δ. The inset shows the fit of Dynes function (blue curve) to our normalized $\mathrm{d}I/\mathrm{d}V$ data at 17 K (black open circles).

ordered atomically resolved image. However, it is still possible to position the tip in one crystalline grain and to measure the local spectroscopy. To investigate the spatial dependence of surface DOS, spectral surveys were made, in which the local density of states (LDOS) is measured at a dense array of locations (24 × 24 grids at the same area as the topographic image) in order to map the spatial variations of spectral features. As demonstrated in figure 1(b), the tunneling spectra exhibit a very similar shape across the 15 nm region (see black spots in figure 1(a)). This suggests that the STS is insensitive to the location, given the fact that its in-plane superconducting coherence length is less than 2 nm [13, 20]. Nevertheless, all spectra clearly reveal coherence 'shoulders' and slightly asymmetric background at $T = 15$ K (figure 1(b)). To manifest the gap, we normalize the spectra by computing the ratio of differential to total conductivity, $(\mathrm{d}I/\mathrm{d}V)(I/V)^{-1}$ [21]. Using this method, the normalized spectra will be independent of different tip–sample separations and provide a relatively direct measure of the surface DOS [21]. The result of such analysis applied to the raw data in figure 1(c) (empty circles) is shown as a black curve, which reveals clearly a single-gap feature. Figure 1(d) displays the temperature evolution of the renormalized spectra. Note the development of the coherence peaks with decreasing temperature below T_c (the raw data were acquired by keeping the tip at the same location as the temperature was changed). As the temperature increases, the dip at zero bias is reduced, almost vanishing near 48.2 K.

For each normalized $(\mathrm{d}I/\mathrm{d}V)(I/V)^{-1}$ spectrum, we extract the magnitude of the superconducting energy gap, Δ, by fitting the $(\mathrm{d}I/\mathrm{d}V)(I/V)^{-1}$ curve to the Dynes function [22] for strong-coupled superconductors, convoluted with a Gaussian distribution to take into account the instrumental resolution and thermal broadening. All data reported were measured with a 1 meV root-mean-square (RMS) modulation, therefore blurring our energy resolution by approximately 2.8 meV. An experiment performed at a temperature of 17.4 K gave an energy broadening of $\sim 4k_BT = 5.8$ meV, where the factor of 4 originates from the fact that the Fermi function smears by approximately k_BT on either side of E_F and we have thermal broadening in both the initial and final states. As demonstrated in the inset of figure 2, each fitting reproduces reasonably the experimental spectrum. The temperature dependence of the superconducting gap obtained from our fitting is shown in the main panel of figure 2, which increases with decreasing temperature. Quantitatively, $\Delta(T)$ follows a BCS-like temperature dependence (shown by the red curve) with $\Delta(0) \sim 9.3$ meV. This gives $2\Delta(0)/k_BT_c \sim 4.3$, slightly higher than the BCS value for the weakly-coupled superconductors.

A BCS-like gap $\Delta(T)$ was previously observed in $SmFeAsO_{0.85}F_{0.15}$ polycrystalline sample via the point-contact Andreev-reflection technique (PCART) [23]. The $\Delta(0)$ value is close to the BCS prediction for the weakly-coupled superconductors. For $NdFeAsO_{0.86}F_{0.14}$, our $\Delta(0)$ value is close to that derived from PCART as well [24, 25], but smaller than those from infrared ellipsometry [26] and angle-resolved photoemission spectroscopy [27]. According to [25], an additional gap feature appears around 4–7 meV below 15–20 K. This is not reflected in our spectra (figure 1). For studying multi-band superconductivity, STM is a unique technique that has successfully revealed two-gap features in MgB_2 [28]. At present, it is too soon to draw any conclusion about gap information, due to the lack of orientation dependence of the gap(s). To the best of our knowledge, there is no other STM/S study on this material. The lack of sizable single-crystal samples may hold back the in-depth investigation.

Fortunately, sizable single crystals can be grown for the 122-type (e.g. $BaFe_2As_2$) materials. This provides tremendous opportunities for various studies, and has already generated large database for their physical properties in a short period. However, there still remain many unsolved issues. For example, $BaFe_2As_2$ is known to undergo a structural and magnetic transition at $T_{MS} \sim 140$ K [7], below which a SDW is formed as confirmed by various measurements such as neutron scattering [29]. Modification of the electronic structure is expected below T_{MS}, because there is normally the opening of an energy gap at the Fermi surface. While infrared spectroscopy measurements provide such evidence [30], many other gap-sensitive techniques reveal a gapless feature below T_{MS}. Our STM/S investigation on $BaFe_2As_2$ single crystals comes to the same conclusion. As shown in figures 3(a) and (c), the STM images taken at liquid nitrogen temperature reveal atomic resolution, indicating the extremely clean surface (*ab*-plane). Note that the surface may form so-called $(\sqrt{2} \times \sqrt{2})$R45° (figure 3(a)) or (1 × 2) (figure 3(c)) structure, with respect to the tetragonal structure notation. The $(\sqrt{2} \times \sqrt{2})$R45° structure reflects the orthorhombic bulk structure as explained in [31] but the (1 × 2) structure is due to the surface reconstruction [32]. At present, it is unclear why these two

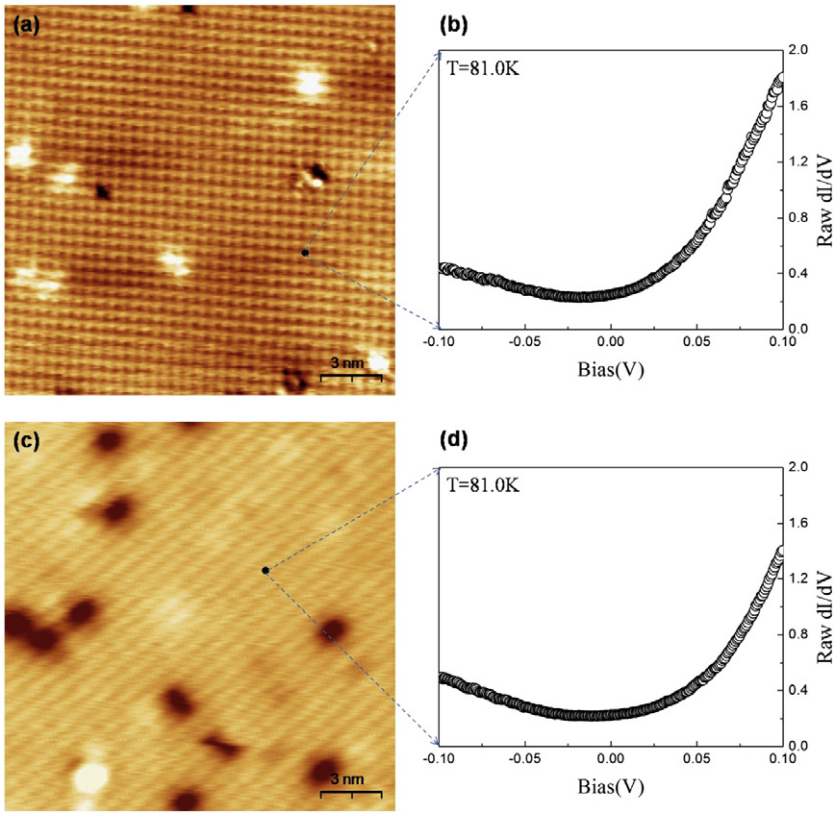

Figure 3. STM images obtained from the surface of $BaFe_2As_2$ single crystal at $T = 81.0$ K revealing two types of structure: (a) $\sqrt{2} \times \sqrt{2}$ and (c) 1×2. The images were taken with the constant current (100 pA); (b) and (d) are tunneling spectra taken in the locations as indicated in (a) and (c).

types of structure coexist. Nevertheless, the STS data obtained from these two types of surface give qualitatively the same spectra, without any gap feature between −100 and +100 meV (see figures 3(b) and (d)). The temperature evolution of STS spectra may provide useful information, and help explain the better electrical conduction below T_{MS} [7].

2.2. High-temperature magnetic susceptibility of $BaFe_2As_2$ and $SrFe_2As_2$ single crystals

In addition to the above-mentioned unusual temperature dependence of the electrical resistivity, the magnetic susceptibility (χ) of $BaFe_2As_2$ seems also to behave unconventionally, as pointed out by Sales *et al* [18]. Above T_{MS}, it is expected to exhibit paramagnetic behavior and follow the Curie–Weiss-like temperature dependence. The data shown in [18] indicate an opposite trend. We therefore measured the magnetic susceptibility of $BaFe_2As_2$ and $SrFe_2As_2$ single crystals over a much extended temperature range. Shown in figure 4 is χ versus T for $BaFe_2As_2$ and $SrFe_2As_2$ between 2 and 700 K. The data were taken in both warming up and cooling down cycles, so as to ensure the stability of the sample in the measured temperature range. Above ∼700 K, the difference between χ_{warm} and χ_{cool} develops slowly for either $BaFe_2As_2$ or $SrFe_2As_2$, suggesting the possible decomposition of the sample. The linear behavior of $\chi(T)$ is very similar to that observed in Cr [33], another SDW system. For direct comparison, we also measured the magnetic susceptibility of a

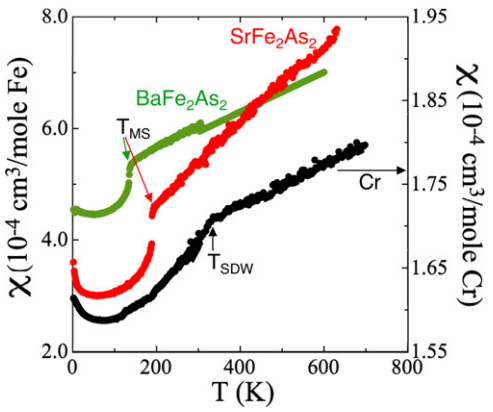

Figure 4. Temperature dependence of the magnetic susceptibility for $BaFe_2As_2$ (green circles), $SrFe_2As_2$ (red circles), and Cr (black circles). All data were measured by applying 1 T DC magnetic field ($H = 1$ T) in both SQUID and vibrating sample magnetometers in order to cover the wider temperature range. For both $BaFe_2As_2$ and $SrFe_2As_2$ single-crystal samples, H was applied in parallel to their ab-plane direction.

Cr polycrystalline sample (Alfa Aesar 99.999%). Remarkably, it represents all features seen in Fe-based parent compounds, where the anomaly corresponds to the SDW transition at $T_{Cr} \sim$ 310 K [34]. It was proposed that the unusual high-temperature susceptibility results from the multi-band nature of Fe-based compounds [18]. Interestingly, Cr is also a multi-band system,

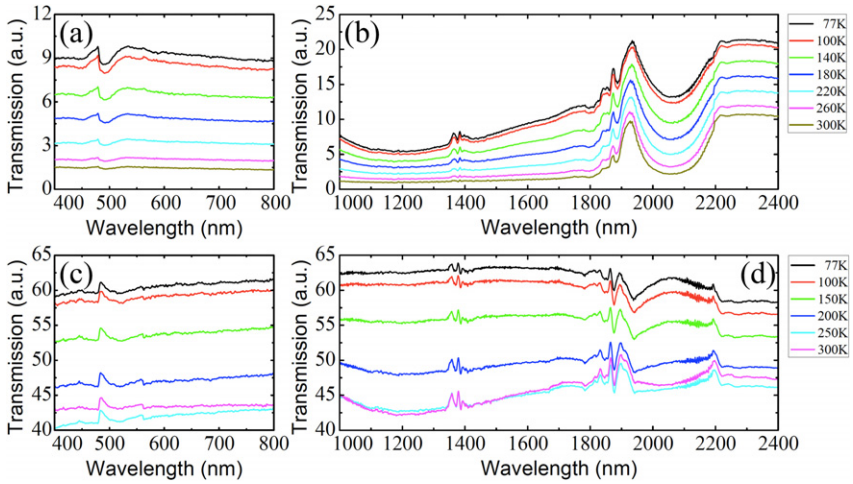

Figure 5. Optical transmission spectra for $BaFe_2As_2$ (thickness of 0.3 mm) ((a) and (b)) and $Ba(Fe_{0.9}Co_{0.1})_2As_2$ (thickness of 0.1 mm) ((c) and (d)) with the wavelength in the range of 400–2400 nm at the indicated temperatures.

consisting of both electron and hole Fermi surfaces. The origin of the SDW in Cr was believed to result from the pairing of electrons and holes with opposite spin [35]. However, when debating whether the SDW is driven by the same mechanism in Fe-based parent compounds and Cr, it should be realized that differences exist between two systems. For example, in Cr, there is clearly an opening of a gap at the Fermi surface when the SDW is formed. Correspondingly, the electrical resistivity increases abruptly at the transition [34].

2.3. Optical transmission spectra of $BaFe_2As_2$ and $Ba(Fe_{0.9}Co_{0.1})_2As_2$ single crystals

To understand issues discussed above, we measured the optical transmission spectroscopy of $BaFe_2As_2$ (with thickness of 0.3 mm) and $Ba(Fe_{1.9}Co_{0.1})_2As_2$ (with thickness of 0.1 mm) single crystals. The transmission spectra were measured using a PerkinElmer Lambda 900 spectrophotometer in the wavelength range from 400 to 2400 nm when the incident beam is perpendicular to the *ab*-plane of the crystals. The samples were fixed in the liquid nitrogen optical spectroscopy cryostat (OXFORD instruments, Optistat® DN) with the temperature varying from 77 to 300 K. The sample was sandwiched by two glass slides, fixed on the end of a long steel stick (∼30 cm long), then inserted into the cryostat. The spectrometer was set for transmission mode with the spot size of 5% with an area of 1.5 mm × 1.0 mm, and the cryostat was put into the spectrometer properly so that the light beam was just on the sample. The normal transmission spectra were measured by the spectrometer, with the temperature tuned from 77 to 300 K.

Figures 5(a) and (b) show the transmission spectra of $BaFe_2As_2$ in the visible (400–800 nm) and near-infrared region (1000–2400 nm) at temperatures of 77, 100, 140, 180, 220, 260 and 300 K. The spectrum in the visible region is nearly constant except for a small bend around 500 nm. As the temperature increases, it decreases gradually from ∼9% at 77 K to ∼1.5% at 300 K. In the near-infrared region, there is a peak at 1930 nm followed by a dull dip centered at 2060 nm, and the transmission rate at short wavelength is lower than that at long wavelength. As the temperature increases from 77 to 300 K, the transmission decreases by ∼6% at short wavelength and ∼10% at long wavelength, respectively. Nevertheless, the spectra remain qualitatively the same above and below T_{MS}. The lack of response to the magnetic/structural transition is again surprising, as the OTS is usually sensitive to both crystallographic and electronic changes.

To help understand OTS of $BaFe_2As_2$, we further measured transmission spectra of $Ba(Fe_{0.9}Co_{0.1})_2As_2$, which is the optimally doped superconductor. Figures 5(c) and (d) show the transmission spectra of $Ba(Fe_{0.9}Co_{0.1})_2As_2$ in the visible and near-infrared region at the indicated temperatures. Similar to that for the parent $BaFe_2As_2$, the spectrum in the visible region is flat except for a small bend around 500 nm, and it increases a little with the wavelength. As the temperature increases, it decreases gradually from ∼60% at 77 K to ∼40% at 300 K. In the near-infrared region, the transmission rate at short wavelength is higher than that at long wavelength at 77 K. As the temperature increases from 77 to 300 K, the transmission decreases by ∼20% for short wavelength and ∼12% for long wavelength. Therefore, the transmission at short wavelength becomes lower than that for long wavelength at 300 K. Obviously, the transmission of $BaFe_2As_2$ is much lower than that of $Ba(Fe_{0.9}Co_{0.1})_2As_2$, as the former is much thicker. Comparing the two sets of OTS, we note the major difference occurs in the region between 1900 and 2200 nm: there is a peak at 1930 nm and a dull dip at 2060 nm for $BaFe_2As_2$, but not obvious for $Ba(Fe_{0.9}Co_{0.1})_2As_2$. Note that, in figure 5(d), a peak in the spectra of $Ba(Fe_{0.9}Co_{0.1})_2As_2$ develops when $T < \sim 150$ K. Since there is no evidence for the magnetic/structure transition in OTS of $BaFe_2As_2$, this peak is unlikely due to any subtle change such as magnetic fluctuations and/or structural distortions. Whether this is associated with electronic properties is yet to be investigated.

3. Summary

Several experimental techniques were employed to study the electronic, magnetic, and optical properties of $NdFeAsO_{0.86}$

$F_{0.14}$, $SrFe_2As_2$, $BaFe_2As_2$, and $Ba(Fe_{0.9}Co_{0.1})_2As_2$. Below the superconducting transition temperature, the scanning tunneling spectra of polycrystalline $NdFeAsO_{0.86}F_{0.14}$ reveal single-gap feature. The quantitative fitting of STS data to the Dynes function results in BCS-like temperature dependence of the energy gap $\Delta(T)$, with $2\Delta(0)/k_BT_c \sim 4.3$. Surprisingly, there is no sign of the energy gap opening in the SDW state of $BaFe_2As_2$ according to our STM/S investigation on the clean surface with the atomic resolution. Despite the abrupt change in magnetic susceptibility at the magnetic and structural transition temperature T_{MS}, the optical transmission spectra of $BaFe_2As_2$ remain qualitatively the same above and below T_{MS}. The lack of response in STS and OTS suggests that the underlying physics associated with such magnetic/structural transitions is unconventional. Above T_{MS}, the T-linear dependence of magnetic susceptibility of $BaFe_2As_2$ and $SrFe_2As_2$ may be attributed to their unique electronic structures that have both electron and hole pockets.

Acknowledgments

This research was supported in part (MHP, JFW) by the Laboratory Directed Research and Development Program at Oak Ridge National Laboratory (ORNL), managed by UT-Battelle, LLC for the US Department of Energy (DOE), and in part (ASS, MAM, BCS, DM, JRT) by the Division of Materials Sciences and Engineering (DMS&E), US DOE at ORNL. EWP, XH and GL would like to acknowledge support from the National Science Foundation (NSF) and DOE (DMS&E) through NSF-DMR-0451163 and also the support from The University of Tennessee SARIF program.

References

[1] Kamihara Y, Watanabe T, Hirano M and Hasono H 2008 *J. Am. Chem. Soc.* **130** 3296
[2] Ren Z A *et al* 2008 *Chin. Phys. Lett.* **25** 2215
[3] Rotter M, Tegel M and Johrendt D 2008 *Phys. Rev. Lett.* **101** 107006
[4] Wang X C, Liu Q Q, Lv Y X, Gao W B, Yang L X, Yu R C, Li F Y and Jin C Q 2008 *Solid State Commun.* **148** 538
[5] Hsu F C *et al* 2008 *Proc. Natl Acad. Sci.* **105** 14262
[6] Ogino H, Katsura Y, Horii S, Kishio K and Shimoyama J 2009 *Supercond. Sci. Technol.* **22** 085001
[7] Sefat A S, Jin R, McGuire M A, Sales B C, Singh D J and Mandrus D 2008 *Phys. Rev. Lett.* **101** 117004
[8] Leithe-Jasper A, Schnelle W, Geibell C and Rosner H 2008 *Phys. Rev. Lett.* **101** 207004
[9] Sefat A S, Jin R, McGuire M A, Sales B C, Mandrus D, Ronning F, Bauer E D and Mozharivskyi Y 2009 *Phys. Rev.* B **79** 094508
[10] Schnelle W, Leithe-Jasper A, Gumeniuk R, Burkhardt U, Kasinathan D and Rosner H 2009 *Phys. Rev.* B **79** 214516
[11] Yamamoto A *et al* 2009 *Appl. Phys. Lett.* **94** 062511
[12] Vilmercati P *et al* 2009 *Phys. Rev.* B **79** 220503
[13] Putti M *et al* 2010 *Supercond. Sci. Technol.* **23** 034003
[14] Yuan H Q, Singleton J, Balakirev F F, Baily S A, Chen G F, Luo J L and Wang N L 2009 *Nature* **457** 565
[15] Mazin I I, Singh D J, Johannes M D and Du M H 2008 *Phys. Rev. Lett.* **101** 057003
[16] Kuroki K, Onari S, Arita R, Usui H, Tanaka Y, Kontani H and Aoki H 2008 *Phys. Rev. Lett.* **101** 087004
[17] Ding H *et al* 2008 *Europhys. Lett.* **83** 47001
[18] Sales B C, McGuire M A, Sefat A S and Mandrus D 2010 *Physica* C **470** 304
[19] Zuev Y L, Specht E D, Cantoni C, Christen D K, Thompson J R, Jin R, Sefat A S, Mandrus D G, McGuire M A and Sales B C 2009 *Phys. Rev.* B **79** 224523
[20] Wang X, Ghorbani S R, Peleckis G and Dou S 2009 *Adv. Mater.* **21** 236
[21] Stroscio J A, Feenstra R M and Fein A P 1986 *Phys. Rev. Lett.* **57** 2579
[22] Dynes R C, Narayanamurti V and Garno J P 1978 *Phys. Rev. Lett.* **41** 1509
[23] Chen T Y, Tesanovic Z, Liu R H, Chen X H and Chien C L 2008 *Nature* **453** 1224
[24] Yates K A, Cohen L F, Ren Z-A, Yang J, Lu W, Dong X-L and Zhao Z-X 2008 *Supercond. Sci. Technol.* **21** 092003
[25] Samuely P, Szabó P, Pribulová Z, Tillman M E, Bud'ko S L and Canfield P C 2009 *Supercond. Sci. Technol.* **22** 014003
[26] Dubroka A, Kim K W, Rössle M, Malik V K, Drew A J, Liu R H, Wu G, Chen X H and Bernhard C 2008 *Phys. Rev. Lett.* **101** 097011
[27] Kondo T *et al* 2008 *Phys. Rev. Lett.* **101** 147003
[28] Iavarone M, Karapetrov G, Koshelev A E, Kwok W K, Crabtree G W and Hinks D G 2002 *Phys. Rev. Lett.* **89** 187002
[29] Huang Q, Qiu Y, Bao W, Green M A, Lynn J W, Gasparovic Y C, Wu T, Wu G and Chen X H 2008 *Phys. Rev. Lett.* **101** 257003
Wilson S D, Yamani Z, Rotundu C R, Freelon B, Courchesne E B and Birgeneau R J 2009 *Phys. Rev.* B **79** 184519
[30] Hu W Z, Zhang Q M and Wang N L 2009 *Physica* C **469** 545
[31] Nascimento V B *et al* 2009 *Phys. Rev. Lett.* **103** 076104
[32] Chuang T M *et al* 2010 *Science* **327** 181
[33] Kittel C 1996 *Introduction to Solid State Physics* 7th edn (Hoboken, NJ: Wiley) p 437
[34] Fawcett E 1988 *Rev. Mod. Phys.* **60** 209
[35] Overhauser A and Arrott A 1960 *Phys. Rev. Lett.* **4** 226
Overhauser A W 1962 *Phys. Rev.* **128** 1437